

# High Intensity Cyclotron Simulations: Towards Quantitative Predictions

Andreas Adelman<sup>\*</sup>, S. Adam, M. Humbel, P.A. Schmelzbach, PSI, Switzerland

## Abstract

PSI operates the most powerful cyclotron worldwide to the benefit of a multi-user, cross-disciplinary research facility. The accelerator complex consists of a Cockcroft-Walton pre-injector, a 72-MeV separated sector injector cyclotron and a 590-MeV separated sector Ring Cyclotron. A beam current of 1.9 mA is routinely extracted from the Ring Cyclotron overall absolute losses are below 1E-3. The facility has a considerable potential for further improvements, an ongoing upgrade project aims at a beam current of 3 mA [2, 1]. The purpose of our multi-scale three-dimensional parallel code and methods development is to make the step from qualitative to quantitative predictions. Their simulation requires the accurate three-dimensional modeling of large and complicated accelerator structures including space charge, beam lines, collimation, and in the future secondary effects. We will show methods, both numerically and computational, that we use presently and give an overview on future directions. Measurements from the cyclotrons and beamlines will be compared with simulations carried out in the frame of the high intensity upgrade program.

## GOALS

Our primary goal, quantitative prediction from the point of particle loss prediction must be viewed from two different viewpoints:

- controlled losses
- uncontrolled losses.

With controlled losses we understand particle losses in special areas of the machine mainly injection and extraction. These areas are heavy shielded and remote handling is possible. The total controlled losses is in the order of  $10^{-3}$ . The uncontrolled losses on the other hand is in the order of nano ampere per meter or 0.5 W/m.

We define *precise beam dynamics simulation* with the ability to perform simulations with enough accuracy i.e. statistics to predict the above mentioned losses in our machines.

In this discussions we do not cover other important problem complexes such as the interaction between high intense beams, rf and high voltage devices or secondary emission problems. We also restrict us to single bunch simulations in the cyclotrons. A more complete discussion on our modeling efforts can be found in a recent ICFA BD-Newsletter [4].

<sup>\*</sup> andreas.adelman@psi.ch

## MAD9P

MAD9P (Methodical Accelerator Design version 9 - parallel) is a general purpose parallel particle tracking program including three-dimensional space charge calculation [3].

## Mathematical and Physical Model

MAD9P is based on the Vlasov-Maxwell equations. In this model, particle motion is governed by external fields and a mean-field approach for the space-charge fields. Particle collisions and radiation are neglected. The total Hamiltonian for a beam line element can be written as a sum of two parts,  $\mathcal{H} = \mathcal{H}_1 + \mathcal{H}_2$ , which correspond to the external and space charge contributions. A second-order integration algorithm (split operator) for a single step is then given by

$$\mathcal{M}_k(\tau) = \mathcal{M}_k^1(\tau/2) \mathcal{M}_k^2(\tau) \mathcal{M}_k^1(\tau/2) + \mathcal{O}(\tau^3) \quad (1)$$

where  $\tau$  denotes the step size,  $\mathcal{M}_k^1$  is the map corresponding to  $\mathcal{H}_1$  obtained by differential algebra methods from a general relativistic Hamiltonian and  $\mathcal{M}_k^2$  is the map corresponding to  $\mathcal{H}_2$ .  $\mathcal{M}_k^2$  is obtained by discretizing the resulting Poisson problem on a rectangular mesh using Fourier techniques, as described in the second section of this paper. Open and periodic boundary conditions can be chosen. Once the physical elements are put together in an arbitrary way the elements are assumed to be perfectly aligned. To

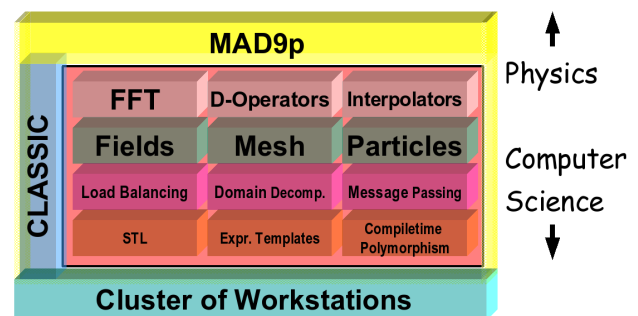


Figure 1: Color: Design of MAD9P

every beam element belongs a corresponding transfer map  $\mathcal{M}_k^2$  which maps every initial condition  $\zeta^i$  of the six dimensional phase space onto a final condition  $\zeta^f$  by

$$\zeta^f = \mathcal{M}_k^2 \zeta^i. \quad (2)$$

MAD9P derives  $\mathcal{M}^2$  by a *Lie algebraic method*. The fact that the negative Poisson bracket of the Hamiltonian and

the density function  $f$  is just the derivative of the density function with respect to the time leads to

$$f(t) = e^{-[t, \mathcal{H}_2]} \cdot f(0). \quad (3)$$

$e^{[t, \mathcal{H}_2]}$  corresponds to  $\mathcal{M}^2$  which can now be expanded in a Taylor series.

Next we show three applications with results, all the way from the 870 keV injection line to the first turns of Injector 2 including the buncher and collimation.

### Construction Principals and Scalability of MAD9P

MAD9P was designed from the beginning with large scale problems in mind. The core frameworks are CLAS-SIC, providing the physics and IPPL (Independent Parallel Particle Layer) which provides data parallel operators on particles and Cartesian meshes. Figure 1 shows the relevant building blocks of MAD9P and the design philosophy, which strictly separates Physics and (parallel) Computer Science. Figure 2 shows the scalability of MAD9P for a

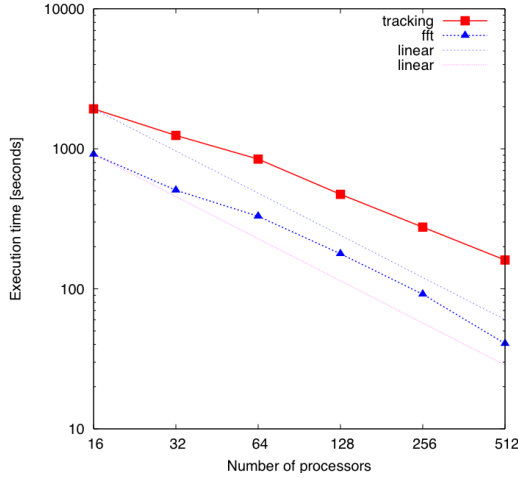


Figure 2: Color: Scalability of MAD9P

test example a beam in a drift tube with a Gaussian particle distribution. The red line shows the total time and the blue line the time for the 3D FFT. The dotted line shows the linear speedup.

## SIMULATIONS

### B870 Injection Line

The starting point for all calculations is the B870 injection line shown in Figure 3. A 4-dimensional transverse phase space distribution, which has been proven to be physically satisfactory in the daily operation of the beam line is used. The longitudinal dimensions are uniform in space and momenta. The initially DC beam is modeled by using a characteristic longitudinal beam length of  $\beta\lambda$ , where  $\lambda$  is the wave length of the RF. The double gap buncher is

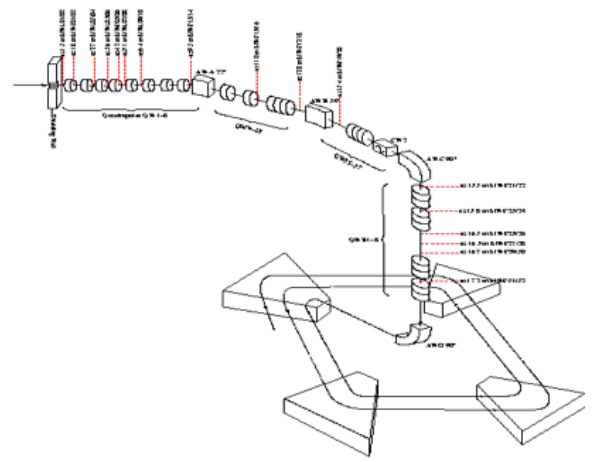


Figure 3: Color: B870 injection line layout showing all profile monitor locations

modeled by (analytic) sinusoidal momenta modulation of the beam. Fig. 4 shows the horizontal beam envelope (similar results are obtained in the vertical direction after fitting the 4-dimensional transverse distribution and a global space-charge neutralisation factor  $f_e$  using a stochastic fit

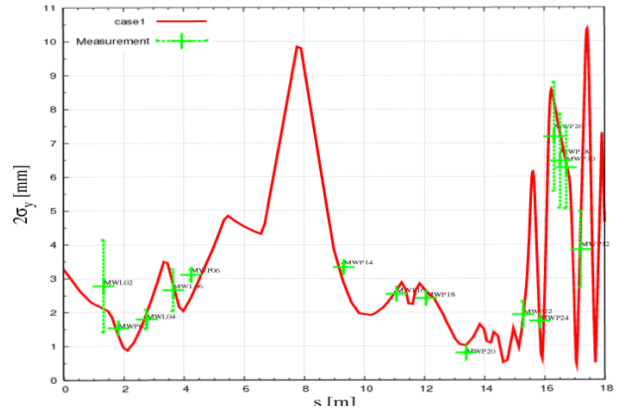


Figure 4: Color: Vertical beam profiles

algorithm based on Simulated Annealing. Define  $F$  as,

$$F = \sum_{n=1}^{\#monitors} (X_{mea}(s_n) - X_{sim}(s_n))^2, \quad (4)$$

this function is a measure of the degree of conformity between simulation and profile monitor measurements, where  $X_{mea}(s_n)$  is a measured rms quantity at the position  $s_n$  along the beam line as shown in Figure 3.  $X_{sim}(s_n)$  is the corresponding calculated quantity obtained by MAD9P. The fitting procedure then minimizes  $F$  in Eq. (4). As shown in Figure 4 we obtain good agreement between measurement and simulation. The space-charge neutralisation factor  $f_e = 0.59$  obtained is in the expected range (for reference see [3]). The error bars in Figure 4 shows the differences between raw measurement data and the measurement data which are filtered based on the level of noise

in the tails of the distribution. In Figure 5 two measured profiles (black) and the corresponding data from the simulation (red) are shown. We note the very good agreement even the complicated hollow profile obtained in the vertical section of the B870 injection line is very well reproduced by the simulation.

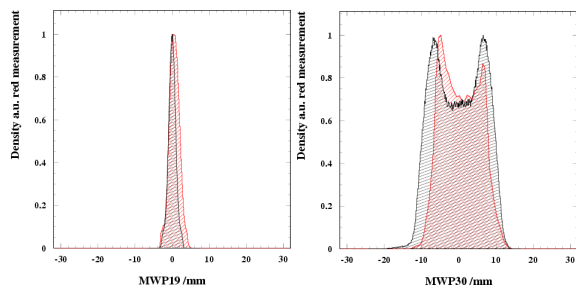


Figure 5: Color: Profiles

### Collimation in the Injector 2 Central Region

The simplified central region of the Injector 2 cyclotron is shown in Figure 6. After lengthy precision work on positioning the collimators and fine-tuning the details of the injection, we were able to simulate the very beginning of Injector 2 with satisfactory results. The z-axis is the direc-

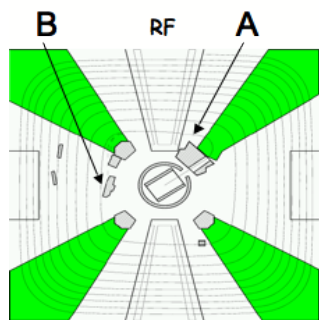


Figure 6: Color: Injector 2 simplified central region collimator scheme

tion of beam propagation and the x-axis points to the center of the cyclotron. Looking at Figure 7 and Figure 8 makes it clear that the bunch center rotates itself, the lower arm is expanding and the bunch has been collimated at the right place (point B in Figure 6).

The amount of beam deposition on the collimators in the central region are well in agreement with observation, we agree in the order of 10 % with respect to measurements.

### CONCLUSIONS

The focus on our beam dynamics code and methods development is on the quantitative modelling of large and complicated accelerator structures. This can be achieved by combining latest numerical and computational methods such as state-of-the-art parallel Particle-In-Cell (PIC),

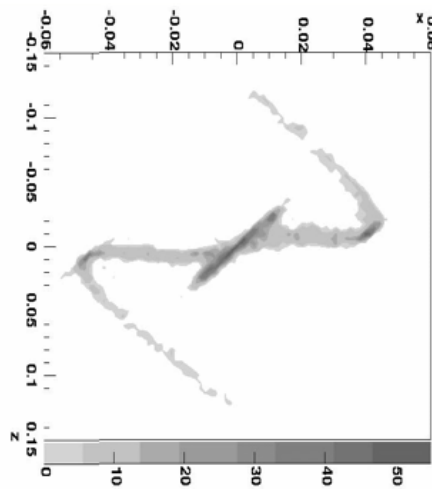


Figure 7: Charge density (a.u.) of the proton beam at point A after the last 90 degree bending magnet of the B870 beam line

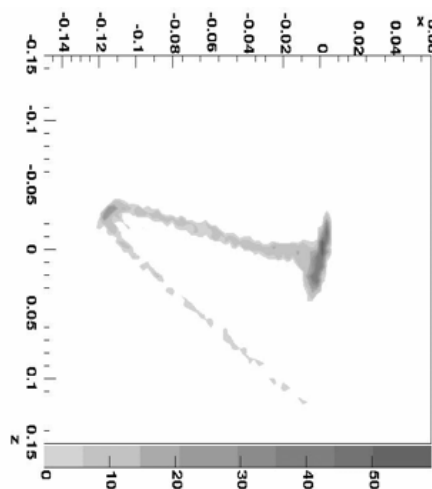


Figure 8: Charge density (a.u.) of the proton beam at point B after passing the tow collimators KIP1 and KIP2

as well as large-scale parallel computing capabilities. We need *precise beam dynamics simulation* in order to perform simulations with enough accuracy i.e. statistics to predict losses in the order of 0.5 W/m in our machines.

### REFERENCES

- [1] P.A. Schmelzbach, "Experience with high-power operation of the PSI proton accelerator facility", HB2006, THAZ01
- [2] H.R. Fitze, "Developments at PSI (including new RF cavity)" Cyclotrons 2004.
- [3] A. Adelman, "3D Simulations of Space Charge Effects in Particle Beams", PhD Thesis, ETH Zurich (2002).
- [4] A. Adelman et.al, "Beam Dynamic Activities at PSI's High Intensity Cyclotrons ", ICFA BD-Newsletter No. 37, August 2005